TISSUE ENGINEERING: Part A
Volume 00, Number 00, 2011

DOI: 10.1089/ten.tea.2011.0032

**Original Article**

# Discontinuous Release of Bone Morphogenetic Protein-2 Loaded Within Interconnected Pores of Honeycomb-Like Polycaprolactone Scaffold Promotes Bone Healing in a Large Bone Defect of Rabbit Ulna

Ji-Hoon Bae, M.D., Ph.D.,[1] Hae-Ryong Song, M.D., Ph.D.,[2] Hak-Jun Kim, M.D., Ph.D.,[2] Hong-Chul Lim, M.D., Ph.D.,[2] Jung-Ho Park, M.D., Ph.D.,[1] Yuchun Liu, Ph.D.,[3] and Swee-Hin Teoh, Ph.D.[3]

The choice of an appropriate carrier and its microarchitectural design is integral in directing bone ingrowth into the defect site and determining its subsequent rate of bone formation and remodeling. We have selected a three-dimensional polycaprolactone (PCL) scaffold with an interconnected honeycomb-like porous structure to provide a conduit for vasculature ingrowth as well as an osteoconductive pathway to guide recruited cells responding to a unique triphasic release of osteoinductive bone morphogenetic proteins (BMP) from these PCL scaffolds. We hypothesize that the use of recombinant human bone morphogenetic protein 2 (rhBMP2)-PCL constructs promotes rapid union and bone regeneration of a large defect. Results of our pilot study on a unilateral 15 mm mid-diaphyseal segmental rabbit ulna defect demonstrated enhanced bone healing with greater amount of bone formation and bridging under plain radiography and microcomputed tomography imaging when compared with an empty PCL and untreated group after 8 weeks postimplantation. Quantitative measurements showed significantly higher bone volume fraction and trabecular thickness, with lower trabecular separation in the rhBMP2-treated groups. Histology evaluation also revealed greater mature bone formation spanning across the entire scaffold region compared with other groups, which showed no bone regeneration within the central defect zone. We highlight that it is the uniqueness of the scaffold having a highly porous network of channels that promoted vascular integration and allowed for cellular infiltration, leading to a discontinuous triphasic BMP2 release profile that mimicked the release profile during natural repair mechanisms *in vivo*. This study serves as preclinical evidence demonstrating the potential of combining osteoinductive rhBMP2 with our PCL constructs for the repair of large defects in a large animal model.

## Introduction

Autologous bone grafts are considered the gold standard for bone replacement as they provide a familiar environment of osteoconductive matrix, osteogenic cells, and osteoinductive signaling molecules necessary for bone regeneration.[1] However, there are disadvantages using autologous bone grafts, such as limited availability of donor tissue and the need for a second surgery, the latter resulting in pain and additional cost. Bone tissue engineering strategy has emerged as an alternative strategy and much research has been focused on designing artificial bone graft substitutes using suitable scaffolds.[2] To attain success in this strategy, one crucial criterion is the microarchitecture of the scaffold. It should mimic the interconnected porous structure of the natural trabecular tissue,[2] which would aid in cell ingrowth and vascularization, thus facilitating host tissue integration and remodeling.[3,4] Bone regeneration is further enhanced by the stiffness matching of the scaffold to the host bone, which provides efficient mechanoinduction for cells to express the extracellular matrix, laying down the appropriate collagen type at the defect zone with respect to the stress environment created by the scaffold.[4] Autologous bone marrow aspirates have been used together with synthetic scaffolds for the repair of nonunion long bone fractures[4] because of their rich source of osteogenic precursors[5–7] that secrete cytokines such as bone morphogenetic protein (BMP), which promotes bone healing.[8,9] However, problems of necrosis at the central core

[1]Department of Orthopaedic Surgery, Korea University Ansan Hospital, Ansan Si, Gyeonggi Do, Korea.
[2]Department of Orthopaedic Surgery, Korea University College of Medicine, Guro Hospital, Guro Gu, Seoul, Republic of Korea.
[3]National University of Singapore Tissue Engineering Program (NUSTEP), Centre for Biomedical Materials Applications and Technology (BIOMAT), Department of Mechanical Engineering, National University of Singapore, Singapore, Singapore.

often remains to be the main clinical challenge for the repair of large defects because of insufficient vascular invasion, and implanted cells nearer the central defect zone often have to rely on vasculature confined to the outer graft site to maintain its survival.[4] Thus, the microarchitectural design of the scaffolds is one of the key factors in ensuring the success of bone tissue engineering approaches.

To further enhance bone regeneration, many research groups have reported success in their utility of BMPs as therapeutic agents in combined use with various scaffolds.[10–16] BMPs are cytokines naturally found in the bone matrix and are well known for their osteoinductive capabilities.[11,12] Since the discovery of osteogenic proteins by Urist,[13,14] many follow-up studies have identified the importance of BMPs and its role in bone formation and healing.[15] Experimentally, their use has been widely demonstrated in various ectopic[12,16] and segmental fracture models in rabbits, dogs, and sheep,[17–19] e.g., to induce bone formation and promote rapid healing. Of date, only BMP2 and BMP7 have been approved by FDA for limited clinical use in applications such as spinal fusion and treatment of long bone defects and nonunions.[20] A randomized trial of 450 patients with open tibia fractures showed accelerated bone growth and wound healing and reduced infections with an increased dosage of recombinant human bone morphogenetic protein 2 (rhBMP2) when compared with the controls using an intramedullary nail fixation alone at the end of 12 weeks.[21] In another clinical trial consisting of 124 tibia nonunions, Friedlaender *et al.* demonstrated successful healing when an intramedullary rod was implanted with either BMP-7-collagen–based systems or autografts, showing no significant differences between the two groups at the end of 9 months.[22] Although these products have shown evident success in clinical trials for long bone repair and regeneration, the collagen-based sponges itself are less effective in providing structural integrity and effective mechanoinduction properties in large nonunions sites. An alternative carrier system for the delivery of BMP should be considered.

The purpose of this study was to investigate the efficacy of the three-dimensional (3D) biodegradable porous honeycomb-like polycaprolactone (PCL) scaffold uniquely designed for accelerating bone healing. The specific details of the microarchitectural design of the scaffold is as described in the patent WO/2010/044758 filed in October 2009 for bone tissue applications. Briefly, the highly porous interconnected network facilitates the infiltration of cells and allows for efficient mass transport of nutrients and waste,[23] while promoting vascular penetration and communication through its interconnected channels. Its use has been also reported with much success in a number of clinical trials.[24,25] The continuous filament of the PCL scaffold provides mechanoinductive effects and has osteoconductive influences for guiding bone regeneration through its honeycomb-like microarchitecture.[26,27] Its biodegradability and slow rate of degradation[22,28] is also essential for long-term efficacy during bone regeneration. It provides initial mechanical support to the defect site to withstand load-bearing applications and *in vivo* stresses until it is degraded and gradually replaced with host tissue,[29] while controlling the release of embedded growth factors packed within its uniquely designed central channel.[4] The unique design of a central channel and its multiple side channels creates a stiff but fracture-resistant property that makes it well suited to resist bending, compressive, and torsional forces in bone tissue applications. This is the first time we are reporting the use of this uniquely designed scaffold with BMP2 in a large animal model for long bone repair.

We hypothesize that rhBMP2 therapy delivered through the PCL scaffold would accelerate bone healing in the segmental defect of rabbit ulna, thus serving as a "smart" scaffold to direct vasculature and bone formation along the microarchitectural conduit of the scaffold for efficacious repair of large long bone defects.

## Materials and Methods

### *Experimental design*

All animal experimental procedures were performed under the guidelines for animal scientific procedures approved by the institution's ethical committee. Fifteen skeletally mature male New Zealand white rabbits (age 14–16 weeks, body weight 3.0–3.5 kg) were used for the creation of a 15 mm segmental bone defect of the left ulna. The rabbits were randomly assigned to one of three groups, of which Group 1 is an untreated sham group, Group 2 is implanted with an empty PCL scaffold, and Group 3 is implanted with rhBMP2-loaded PCL scaffold ($n = 5$ per group). The rate of bone healing was assessed by plain radiography, quantitative microcomputed tomography (micro-CT) scan, and histology after 8 weeks postsurgery.

### *Scaffold design and fabrication*

PCL scaffolds were fabricated by Osteopore International Pte. Ltd. in a clean room conforming to ISO13485 and gamma sterilized (17–19 Kray). The method of manufacture has been previously reported[22] and is detailed in the patent WO/2010/044758. Briefly, the scaffold is made up of two tubular portions—the inner and outer portion, each consisting of microchannels. Both portions were separately manufactured by extrusion layer by layer of PCL to form a 3D scaffold. The 3D scaffold was made from microfilaments laid in layers in different angles for each layer to form interconnected pores. Each scaffold has a lay-down pattern of 0/60/120 degree with porosity of 70% and average pore size of 0.515 mm as determined by micro-CT analysis. The outer portion was then rolled upon the inner portion. The scaffolds have a compressive modulus of $23.1 \pm 6.16$ MPa and compressive strength of $6.38 \pm 0.82$ MPa. The structure of PCL scaffold is a honeycomb array of interconnected equilateral triangles with regular porous morphology (Fig. 1). For the purpose of this study, the scaffolds were made cylindrical shaped with 15 mm length and 4 mm diameter.

### *Loading of rhBMP2 on PCL scaffold*

The scaffolds were soaked for 3 h at 37°C in phosphate buffer saline prior to the loading of rhBMP2 using fibrin sealant. About 300 μL of 0.15 mg/mL rhBMP2 (Cowellmedi Corp.) was mixed with 200 μL of fibrin sealant before pipetting onto each scaffold, amounting to a total BMP2 dose of 75 μg per animal. It was previously reported that PCL scaffold displayed a loading efficiency of 70% and triphasic burst releases at 2 h, 7 days, and 16 days.[30]

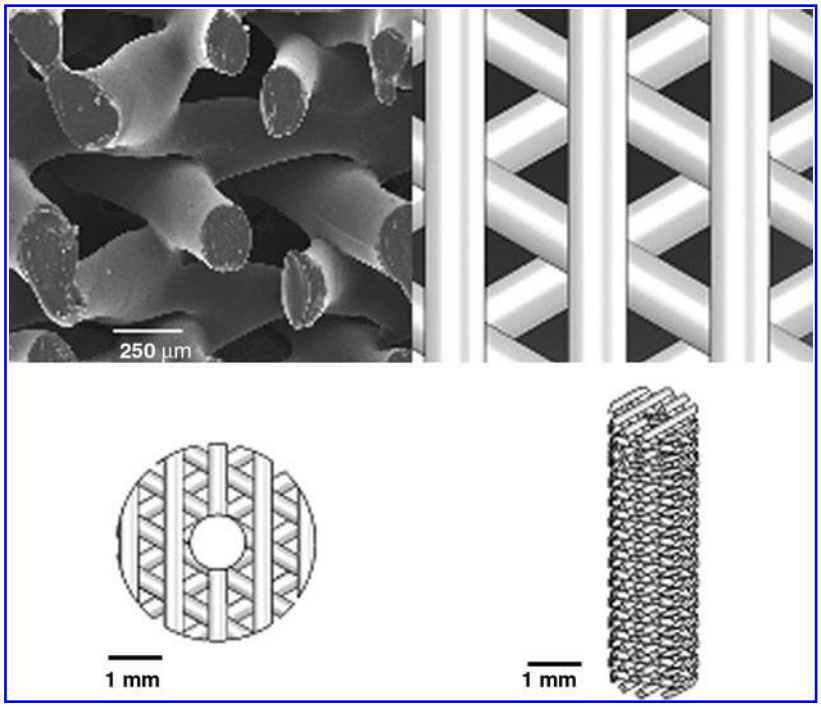


**FIG. 1.** PCL scaffold dimensions measured at all three axes. Scanning electron microscopy and its schematic drawing of microarchitecture of the top and isometric views showed a honeycomb-like structure with a lay-down pattern of 0/60/120 degree with porosity of 70%. PCL, polycaprolactone.

### *Surgical procedure*

The rabbits were anesthetized with an intramuscular injection of ketamine 35 mg/kg and xylazine 5 mg/kg, and left limbs were then shaved and aseptically prepared for surgery. A longitudinal skin incision was made over the ulna and underlying muscles were retracted, exposing the mid-diaphysis of the ulna. Periosteum of operative site was then excised. A 15-mm-length defect was created using a 2.7 mm drill at a distance of 4 cm distal to the olecranon tip using a hand-held osteotome. The ulna bone was removed. The bone defect was lavaged with 0.9% normal saline. The rabbits were randomly assigned to one of three groups: the untreated group (Group 1, $n=5$), a PCL–fibrin scaffold without rhBMP2 treated group (Group 2, $n=5$), and a rhBMP2-loaded PCL–fibrin scaffold treated group (Group 3, $n=5$). The muscle layer and the skin were closed layer by layer after implantation of scaffold constructs. Intramuscular antibiotics were administered twice a day for the first 3 days post-surgery and monitored daily throughout the study, noting a high level of mobility without the need of external support. The animals were euthanized after 8 weeks for post-implantation analysis.

### *Radiographic evaluation*

Anteroposterior and lateral radiographs were immediately taken after surgery and every other month (0, 4, and 8 weeks after surgery). Radiographic evaluation was used to qualitatively estimate bone formation within the defect as well as the timing of callus formation, bridging of defect, corticalization, and recanalization of marrow.

### *Quantitative micro-CT evaluation*

New bone formation was evaluated by the quantitative Micro-CT scan (Skyscan1072; Skyscan) at 8 weeks after surgery. The scanner was set at a voltage of 80 kVp and a current of 100 μA. Resolution was set to "Medium," which created a 1024×1024 pixel image matrix. Isotropic slice data were obtained by the system and reconstructed into 2D images (TomoNT™; Skyscan). These slice images were compiled and analyzed to render 3D images and obtain quantitative architectural parameters. The bone volume fraction (BVF), trabecular thickness (TTh), and trabecular separation (TSp) were quantitatively measured.

### *Histological examination*

Specimens were harvested after 8 weeks and fixed in 10% neutral-buffered formalin for 2 weeks prior to histology processing. Dehydration was accomplished using a graded series of ethyl alcohols (Harleco) and cleared with xylene substitute (Thermo Electron Corporation). Infiltration was then performed using a graded series of methyl methacrylate solutions (ACROS Organics). A catalyzed mixture of Osteo-Bed resin solution containing 2.5 g of benzoyl peroxide (Sigma) per 100 mL was used to embed the specimens and put under vacuum for at least 48 h. After polymerization, specimens were placed in a freezer for 24 h. Specimens were trimmed of excess plastic (Isomet 1000; Buehler), ground to expose relevant portions (Ecomed 3; Buehler), and longitudinally sectioned (3 μm thick) using a microtome (Microm HM355S; Richard Allan Scientific). The specimens were then stained with hematoxylin and eosin and the central region of the defect zone was imaged for new bone formation.

### *Statistical analysis*

One-way analysis of variance was used to analyze the differences in the BVF, TTh, and TSp between the three treatment groups. Values are represented in mean ± standard deviation with a significance level at $p<0.05$ for all analysis. *** indicated $p<0.001$, and ** indicated $p<0.01$.

## Results

### *Radiographic evaluation*

Radiographic evaluation identified new bone formation from either or both ends of the defect in all specimens after 4 weeks of implantation. However, incomplete union persisted in both the empty defect and PCL scaffold group with no or little bone growth at the center of the defect respectively by week 8. Little early-stage bone bridging was seen extending from the proximal end of the femoral defect toward the central region with the implantation of PCL scaffold. Upon loading scaffold with rhBMP2, significant amount of bone ingrowth was seen throughout the implanted scaffold region with extensive amount of bone formed in the defect zone overtime. New cortices were seen extending upward from the distal end by week 4. Bone bridges formed across the distal and proximal end of the defect region, filling the defect zone with dense radio-opaque material and establishing completely union by week 8 (Figs. 2 and 3).

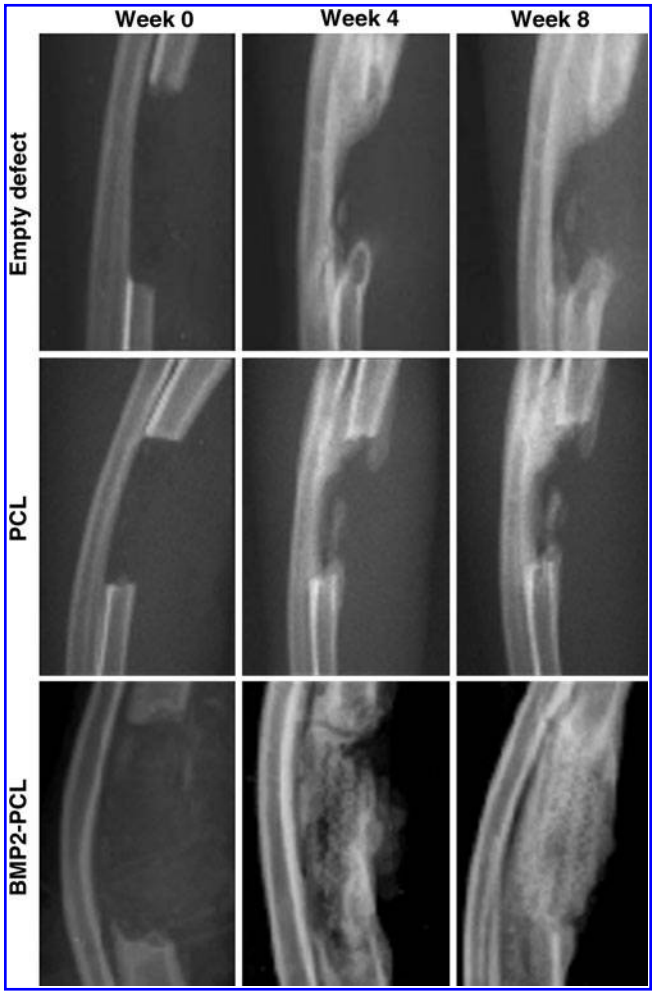


**FIG. 2.** Plain lateral radiographs of all sample groups taken at week 0, 4, and 8 postoperatively. New bone formation was identified from one or both ends of the defect in all specimens by week 4. rhBMP2-treated ulna exhibited greatest amount of bone formation within the defect with bone bridges formed across the entire defect zone but absent in the other groups. rhBMP2, recombinant human bone morphogenetic protein 2.

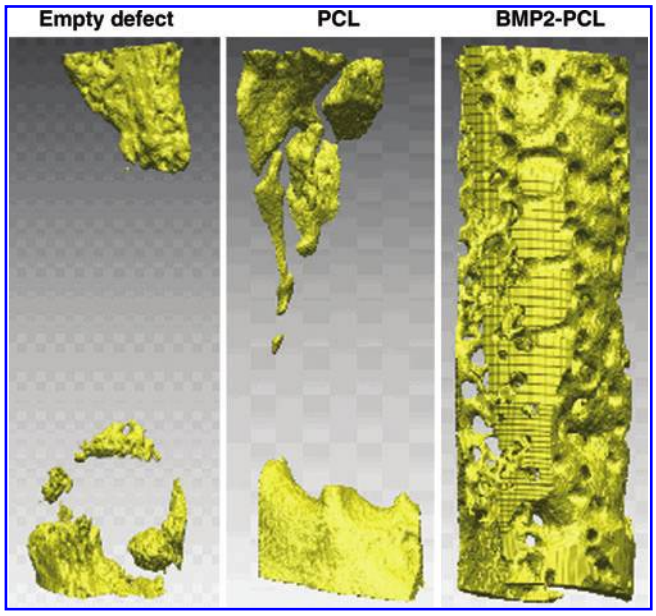


**FIG. 3.** Three-dimensional micro-CT images of all sample groups taken at 8 weeks after surgery. rhBMP2-treated group had greater amount of bone formation than other groups. Bony bridging was observed in the rhBMP2-treated group. micro-CT, microcomputed tomography. Color images available online at www.liebertonline.com/tea

Quantitative assessment of bone quality by micro-CT showed no significant difference between the PCL scaffold and empty defect control groups (Fig. 4b). But, rhBMP2 loaded onto PCL scaffolds showed the formation of dense bone structures, with significantly higher BVF (2.7–3.0× higher; $p < 0.001$) and TTh (2.0–2.1× higher; $p < 0.01$) and with 1.8× decreased TSp ($p < 0.01$) compared with the other groups at week 8 (Fig. 4b).

### *Histological evaluation*

Histology evaluation of the empty defect showed sparse distribution of fibrous connective tissue without any bone formation, whereas the PCL scaffold group exhibited more compact tissue with formation of lamellar bone in the central and proximal regions. The co-implantation of rhBMP2 with PCL scaffold showed extensive formation of bone throughout the entire region of the scaffold (Fig. 5).

## Discussion

In this study, we highlight the importance of an appropriate carrier system for the guidance of cellular ingrowth, vascular penetration, and the delivery of BMP2 for aiding effective bone regeneration and repair of large long bone defects. Consideration factors include its microarchitectural design, porosity, degradation properties, and surface properties, which need to be synchronized with the release profile of the loaded BMP such that it orchestrates the natural bone healing process.[31] In a critical review by Ai-Aql *et al.* entitled "Molecular mechanism controlling bone formation during fracture healing and distraction osteogenesis," the various cytokines including BMPs and their relative expressions during regulation of bone formation was presented.[32] Interesting to note was that the process of distraction osteogenesis

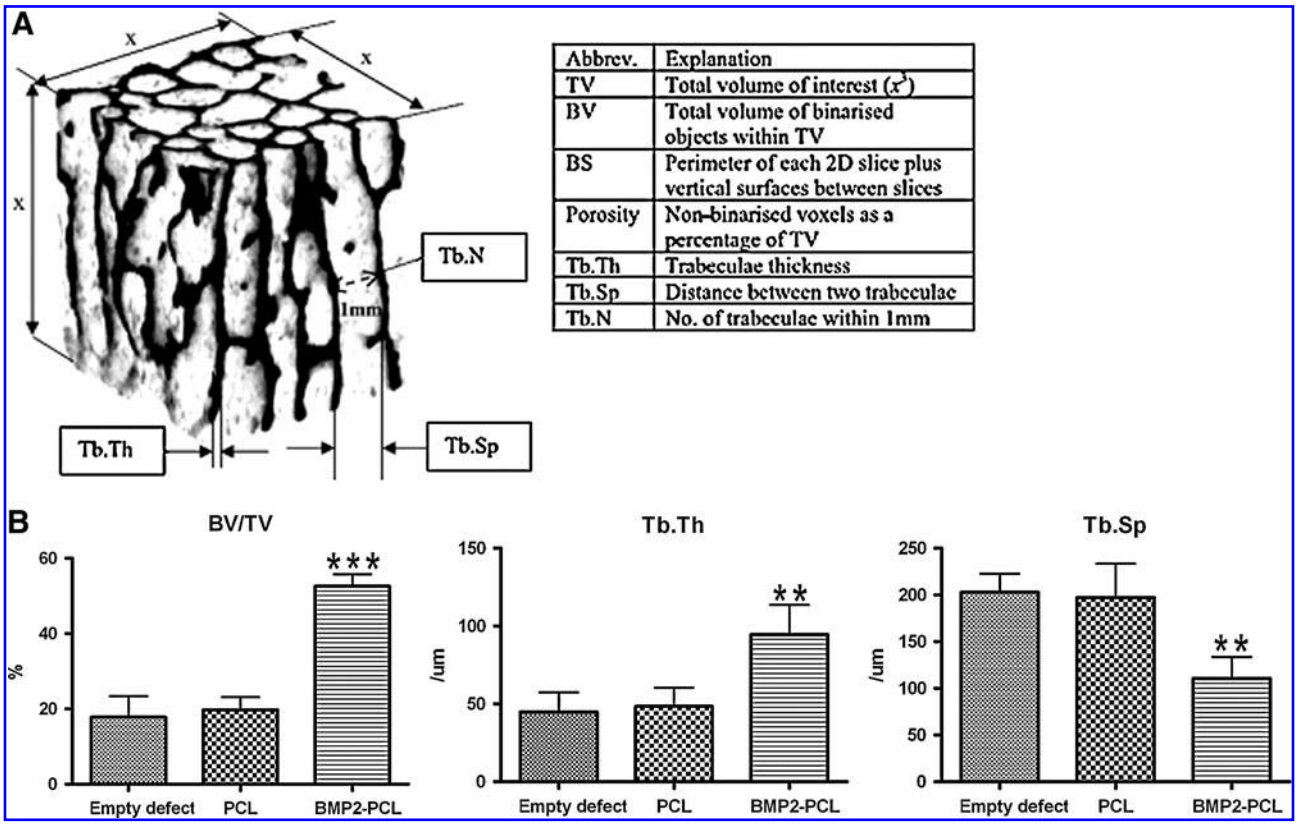


| Abbrev. | Explanation |
|---|---|
| TV | Total volume of interest ($x^3$) |
| BV | Total volume of binarised objects within TV |
| BS | Perimeter of each 2D slice plus vertical surfaces between slices |
| Porosity | Non-binarised voxels as a percentage of TV |
| Tb.Th | Trabeculae thickness |
| Tb.Sp | Distance between two trabeculae |
| Tb.N | No. of trabeculae within 1mm |

**FIG. 4.** **(A)** Schematic diagram of microarchitecture and its associated parameters for evaluating bone from micro-CT images. **(B)** Quantitative micro-CT measured bone volume/total volume of defect (BV/TV), trabecular thickness (Tb.Th), and trabecular separation (Tb.Sp) of all sample groups at week 8 (***$p < 0.001$, **$p < 0.01$).

revealed a noncontinuous production of BMP levels throughout its three temporal and dynamic phases, namely latency, distraction, and consolidation. BMP expression was upregulated during the latent and active distraction phases, but it was downregulated during the consolidation phase. In alignment to this report, our rhBMP-PCL scaffold construct seemingly mimics a similar discontinuous BMP release phenomena via a triphasic release model *in vitro*.

Our previous preliminary work had investigated the *in vitro* release profile of rhBMP2 from PCL scaffolds. It was shown that 10 μg/mL loaded BMP2 had an efficiency of 70%, which demonstrated a unique triphasic release profile with burst release at 2 h and at days 7 and 16[30] (data reproduced in Fig. 6 for ease of reference). Our group is the first group to demonstrate such a unique triphasic rhBMP2 release profile from PCL scaffolds but the actual mechanism has not been fully understood. Rai *et al.* had suggested that the initial burst could be due to rhBMP2 adhesion to the scaffolds through fibrin, and the subsequent rhBMP2 release after fibrin degradation by day 10 could indicate the direct adhesion of the protein onto the PCL scaffolds. The high amount of rhBMP2 retained in the scaffold could also be influenced by the hydrophobic properties of PCL that delayed inward water penetration and slowed down the diffusion of rhBMP-2 out from the scaffold, not commonly seen in other resorbable polymers.[30] We also hypothesize that this discontinuous

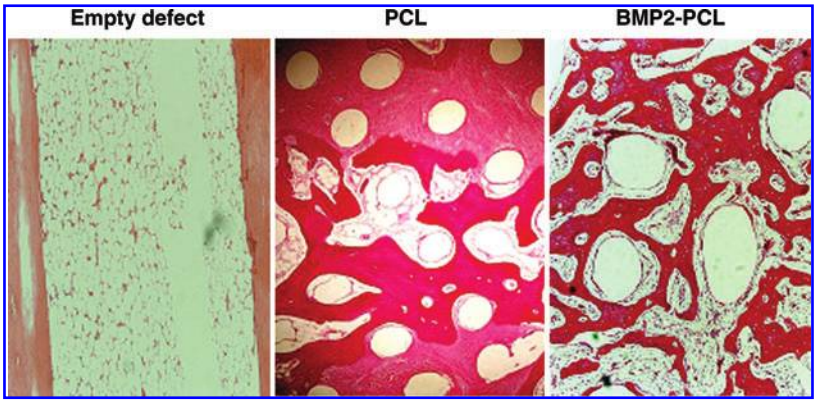


**FIG. 5.** Hematoxylin and eosin staining of the central defect zone at 8 weeks post-surgery (magnification, ×10). The rhBMP2-PCL group showed greater amount of bone formation within the bone defect compared with PCL alone, whereas only sparse connective tissue was present in the empty defect group. Color images available online at www.liebertonline.com/tea

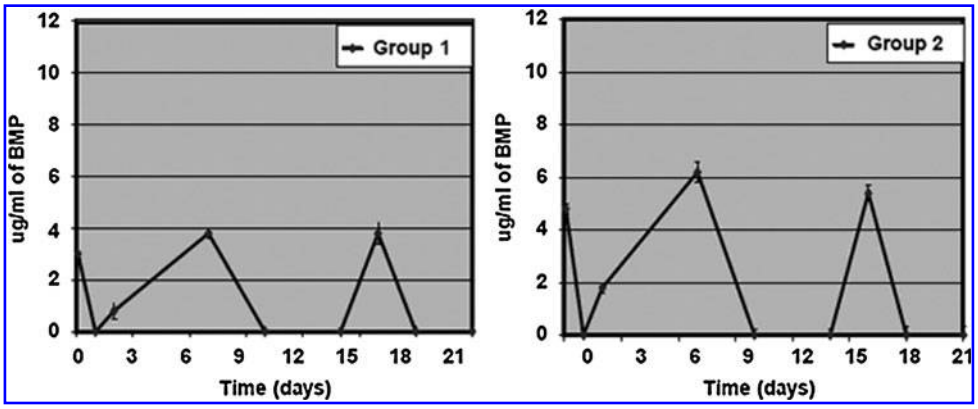


**FIG. 6.** The amount of rhBMP-2 released from PCL–fibrin composites *in vitro* when loaded with 10 μg/mL and 20 μg/mL of rhBMP-2 as a function of time as represented by Groups 1 and 2, respectively. Medium was removed at 2 h, followed by 1, 2, 4, 7, 10, 14, and 21 days, and then quantified by enzyme-linked immunosorbent assay.

release profile and triphasic burst are likely to be associated with the high surface area and unique microarchitecture of the scaffold. Although a direct comparison of the release profile of BMP *in vitro* and *in vivo* cannot be drawn because of the complexities of release patterns within *in vivo* paradigms, the discontinuous BMP2 release from our unique scaffold *in vitro* certainly correlated to the release patterns *in vivo* as described by Ai-Aql,[32] thus suggesting its suitability as a carrier system for BMP for accelerating bone healing.

In our current follow-up study in a long bone rabbit ulna defect model, although the rhBMP2 loading concentration that was used in this study was different, it is expected to exhibit the same release pattern and burst profile, as the dose of BMP2 does not affect the release pattern.[30] It is also important to note that although the optimized rhBMP2 concentrations have to be yet established in this study, its unique triphasic release phenomena from the scaffold closely model the up- and downregulation of BMPs in the natural bone healing processes. The initial burst release of rhBMP2 from PCL–fibrin composites mimics the upregulated endogenous BMP production during the initial phase upon osteotomy, essential for accelerating the osteogenic differentiation of recruited mesenchymal precursor cells to the osteotomized region during intramembranous ossification,[32] thus providing initial stimulus for bone growth. Subsequent downregulation of rhBMP2 release models that of the consolidation phase, as the newly formed bone undergoes extensive mineralization and bone columns interconnect and remodel.

As opposed to most BMP–carrier system studies, various groups have suggested the importance of maintaining a continuous BMP release from the carrier system to induce bone formation. Kempen *et al.* showed a burst release of vascular endothelial growth factor to induce angiogenesis, followed by a sustained release of BMP2 from poly(lactic-*co*-glycolic acid) microspheres embedded in a gelatin hydrogel over 56 days of implantation in rats,[33] whereas Yamamoto *et al.* showed a controlled release of BMP from a gelatin hydrogel with a corresponding enhancement in alkaline phosphatase and osteocalcin levels, suggesting the importance of sustained release for the induction of bone formation.[34] Uludag and coworkers measured the pharmocokinetics of BMP2 release, which demonstrated an initial burst followed by gradual BMP2 loss from the carrier system over time, suggesting the importance of retaining BMP over time for osteoinductive activity of recruited mesenchymal stem cell.[35,36] However, now having understood the molecular signaling expression profile in the natural repair process,[32] we propose future studies to reconsider the traditional hypothesis of a need for a continuous release of BMP as well as the effectiveness of such a release profile for the repair of bone defects and its remodeling process. Further, there is also a fear of inducing tumorigenicity upon sustained release of BMP *in vivo* as a continuous supply of BMP is suggested to be necessary for inducing differentiation of cancer stem cells.[37]

In this study, our results support our hypothesis that rhBMP2 therapy delivered into a PCL scaffold would accelerate healing of the segmental defect compared with the empty defect or implanted PCL scaffold alone. Both radiological and histological evaluation showed that the loading of rhBMP in combination with the PCL scaffold constructs accelerated bone repair, leading to complete union of the defect zone by week 8. We also noted an interesting spatial pattern of bone ingrowth into the scaffolds, which has important implications for ensuring sufficient vascularity and for accelerating bone regeneration. In the PCL scaffold group alone, micro-CT images revealed bone formation initiating from the proximal end toward the midpoint of the defect, suggesting the osteoconductive capabilities of the PCL scaffold in directing host osteoblasts growth through its interconnected porous microarchitecture conduit. The interconnectivity of the porous honeycomb-like network structure of the PCL scaffold allows and guides not only bony ingrowth but also vasculature penetration[38] to maintain survivability of the cells all the way to the center of the large defect zone. These results highlighted the importance of scaffold microarchitecture and its design in providing an osteoconductive path to guide and accelerate bone formation into a 3D form at the defect site.[39,40]

To further enhance the rate of bone regeneration, osteoinductive rhBMP2 was incorporated into the PCL scaffold in this study. rhBMP2 promoted new bone formation and the continuity of bone formed at the host/scaffold interface led to a union repair. The primary mechanism of enhanced healing following rhBMP2 treatment was probably due to an enhanced process of enchondral ossification—rhBMP2 induced the recruitment of native osteoprogenitor cells, promoted chondrogenic differentiation of resident and recruited cells, and facilitated in subsequent cartilage and bone tissue composition.[41–44] The quality of trabecular bone was also dramatically improved as observed from the micro-CT

analysis, noted by the denser bone structures with increased bone volume, greater TTh, and reduced separation of trabecular struts. This result suggests that the addition of rhBMP2 led to the formation of thicker trabecular structures, which forms a sturdier internal architecture of bone, thus providing greater integrity and strength to the newly formed bone. Improved limb functionality of these treated animals is expected, allowing them to withstand greater biomechanical forces during daily loadings. Our findings are consistent with previous studies that showed enhanced bone healing after rhBMP2 treatment, despite differences in the use of animal models, BMP2 doses, and scaffold carriers.[20] For example, Cook *et al.*[17] implanted rabbit bone collagen carrier reconstituted with BMP-7 at a 1.5 cm segmental defect of the rabbit ulna diaphysis. Complete union repair of the defect site with new cortices formation was seen by 8 weeks in all implants with varying concentration of BMP-7, except for those containing 3.13 μg of BMP-7 and empty defect controls. Similar findings were observed when BMP-7 was used in a 2.5-cm-long bone segmental canine defect model and 2 cm ulna defect of nonhuman primates.[18,45]

Our results also showed bone initiation from the ends toward the central core of the defect region rather than ossification from the cortical surface, where the latter is expected to obstruct sufficient nutrients and oxygen supply to the central region of large defects, which results in cellular necrosis. This consideration has been factored in during the design of the scaffold by creating an inner porous portion with microchannel along the plane to provide the initiation site for osteogenesis as outlined in the patent WO/2010/044758. As opposed to cellular engineering therapy, vascular insufficiency at the central core often leads to necrosis as the implanted cells have to rely on the vasculature confined to the outer graft site for cellular survival.[4] Several studies have also shown the importance of vascularization, wherein the rate of bone formation is heavily reliant on the extent of angiogenesis.[46–48] Our findings suggest the importance of an appropriate porous microarchitecture of the scaffold for use in combination with rhBMP2 in directing bone formation while allowing vasculature to penetrate into the central zone, thus allowing rapid healing in 8 weeks and, subsequently, long-term graft survival.

## Conclusion

We highlight our observations on the discontinuous triphasic release pattern of rhBMP2 from our PCL scaffold, which mimicked the BMP expression patterns in natural healing processes, thus playing an important role in coordinating the spatial formation of bone overtime. In this study, the use of osteoinductive rhBMP-2 loaded onto PCL scaffold acted in synergy to recruit, differentiate, and guide host bone ingrowth. Our results demonstrated the effectiveness of honeycomb-like PCL as a carrier for rhBMP2 therapy, which has led to accelerated bone healing in the segmental defect of rabbit ulna when compared with the scaffold and the empty defect groups. The use of PCL as a delivery system for rhBMP2 has proven itself as a favorable osteoconductive support for bony regeneration. As it is biodegradable, it provides initial mechanical strength to support the defect region during neotissue formation before eventually replaced upon degradation, therefore reducing the risk of infections for long-term implantations. Further, PCL has been approved by FDA and the use of a highly reproducible fused deposition modeling technique allows for the precise fabrication of scaffolds based on the micro-CT scans of the defect sites of individuals,[30,38,49,50] thus acting as a promising carrier option for the delivery of BMP in a clinical setting. Our rhBMP2-loaded PCL scaffold in combination serves as a "smart" scaffold, which presents itself as a promising approach for the repair of long bone defects in the clinical realm.

## Acknowledgments

The authors specially thank Hyo-Keun Kim and Mi-Ock Baek for their technical assistance. This research was supported by Basic Science Research Program through the National Research Foundation of Korea funded by the Ministry of Education, Science, and Technology (KRF-2008-313-E00345).

## Disclosure Statement

No competing financial interests exist for all the authors except that Dr. S.H. Teoh and the National University of Singapore are shareholders of Osteopore International (NUS spin-off), which manufactured the scaffolds for this research work. The interpretation of the results was done independently of the company and is the collective view of the rest of the authors. According to the policy of Tissue Engineering, this serves as a disclosure of any conflict of interest whether they are actual or potential by the authors of this manuscript.

## References

1. Horner, E.A., Kirkham, J., Wood, D., Curran, S., Smith, M., Thomson, B., *et al*. Long bone defect models for tissue engineering applications: criteria for choice. Tissue Eng Part B Rev **16,** 263, 2010.
2. Stevens, B., Yang, Y., Mohandas, A., Stucker, B., and Nguyen, K.T. A review of materials, fabrication methods, and strategies used to enhance bone regeneration in engineered bone tissues. J Biomed Mater Res B Appl Biomater **85,** 573, 2008.
3. Mastrogiacomo, M., Scaglione, S., Martinetti, R., Dolcini, L., Beltrame, F., Cancedda, R., *et al.* Role of scaffold internal structure on *in vivo* bone formation in macroporous calcium phosphate bioceramics. Biomaterials **27,** 3230, 2006.
4. Muschler, G.F., Nakamoto, C., and Griffith, L.G. Engineering principles of clinical cell-based tissue engineering. J Bone Joint Surg Am **86-A,** 1541, 2004.
5. Owen, M., and Peck, W. Lineage of osteogenic cells and their relationship to the stromal system. In: Bilezikian, J.P., Raisz, L.G., and Rodan, G.A, eds. Principles of Bone Biology, Volume 1. Irvine, CA: Academic Press, 1985, pp. 1–25.
6. Beresford, J.N. Osteogenic stem cells and the stromal system of bone and marrow. Clin Orthop Relat Res 270, 1989.
7. Friedenstein, A.J. Precursor cells of mechanocytes. Int Rev Cytol **47,** 327, 1976.
8. Southwood, L.L., Frisbie, D.D., Kawcak, C.E., Ghivizzani, S.C., Evans, C.H., McIlwraith, C.W., *et al.* Evaluation of Ad-BMP-2 for enhancing fracture healing in an infected defect fracture rabbit model. J Orthop Res **22,** 66, 2004.
9. Southwood, L.L., Frisbie, D.D., Kawcak, C.E., and McIlwraith, C.W. Delivery of growth factors using gene therapy to enhance bone healing. Vet Surg **33,** 565, 2004.

10. Karageorgiou, V., Meinel, L., Hofmann, S., Malhotra, A., Volloch, V., Kaplan, D., *et al.* Bone morphogenetic protein-2 decorated silk fibroin films induce osteogenic differentiation of human bone marrow stromal cells. J Biomed Mater Res A **71,** 528, 2004.
11. Reddi, A.H., and Cunningham, N.S. Initiation and promotion of bone differentiation by bone morphogenetic proteins. J Bone Miner Res **8 Suppl 2,** S499, 1993.
12. Reddi, A.H. Cell biology and biochemistry of endochondral bone development. Coll Relat Res **1,** 209, 1981.
13. Urist, M.R. Bone: formation by autoinduction. 1965. Clin Orthop Relat Res 4, 2002.
14. Urist, M.R., Mikulski, A., and Lietze, A. Solubilized and insolubilized bone morphogenetic protein. Proc Natl Acad Sci U S A **76,** 1828, 1979.
15. Wozney, J.M., Rosen, V., Celeste, A.J., Mitsock, L.M., Whitters, M.J., Kriz, R.W., *et al.* Novel regulators of bone formation: molecular clones and activities. Science **242,** 1528, 1988.
16. Wang, E.A., Rosen, V., D'Alessandro, J.S., Bauduy, M., Cordes, P., Harada, T., *et al.* Recombinant human bone morphogenetic protein induces bone formation. Proc Natl Acad Sci U S A **87,** 2220, 1990.
17. Cook, S.D., Baffes, G.C., Wolfe, M.W., Sampath, T.K., Rueger, D.C., Whitecloud, T.S., *et al.* The effect of recombinant human osteogenic protein-1 on healing of large segmental bone defects. J Bone Joint Surg Am **76,** 827, 1994.
18. Cook, S.D., Baffes, G.C., Wolfe, M.W., Sampath, T.K., and Rueger, D.C. Recombinant human bone morphogenetic protein-7 induces healing in a canine long-bone segmental defect model. Clin Orthop Relat Res 302, 1994.
19. Gerhart, T.N., Kirker-Head, C.A., Kriz, M.J., Holtrop, M.E., Hennig, G.E., Hipp, J., *et al.* Healing segmental femoral defects in sheep using recombinant human bone morphogenetic protein. Clin Orthop Relat Res 317, 1993.
20. Bessa, P.C., Casal, M., and Reis, R.L. Bone morphogenetic proteins in tissue engineering: the road from laboratory to clinic, part II (BMP delivery). J Tissue Eng Regen Med **2,** 81, 2008.
21. Govender, S., Csimma, C., Genant, H.K., Valentin-Opran, A., Amit, Y., Arbel, R., *et al.* Recombinant human bone morphogenetic protein-2 for treatment of open tibial fractures: a prospective, controlled, randomized study of four hundred and fifty patients. J Bone Joint Surg Am **84-A,** 2123, 2002.
22. Friedlaender, G.E., Perry, C.R., Cole, J.D., Cook, S.D., Cierny, G., Muschler, G.F., *et al.* Osteogenic protein-1 (bone morphogenetic protein-7) in the treatment of tibial nonunions. J Bone Joint Surg Am **83-A Suppl 1,** S151, 2001.
23. Zein, I., Hutmacher, D.W., Tan, K.C., and Teoh, S.H. Fused deposition modeling of novel scaffold architectures for tissue engineering applications. Biomaterials **23,** 1169, 2002.
24. Schuckert, K.H., Jopp, S., and Teoh, S.H. Mandibular defect reconstruction using three-dimensional polycaprolactone scaffold in combination with platelet-rich plasma and recombinant human bone morphogenetic protein-2: *de novo* synthesis of bone in a single case. Tissue Eng Part A **15,** 493, 2009.
25. Schantz, J.T., Lim, T.C., Ning, C., Teoh, S.H., Tan, K.C., Wang, S.C., *et al.* Cranioplasty after trephination using a novel biodegradable burr hole cover: technical case report. Neurosurgery **58,** ONS, 2006.
26. Endres, M., Hutmacher, D.W., Salgado, A.J., Kaps, C., Ringe, J., Reis, R.L., *et al.* Osteogenic induction of human bone marrow-derived mesenchymal progenitor cells in novel synthetic polymer-hydrogel matrices. Tissue Eng **9,** 689, 2003.
27. Hutmacher, D.W., Schantz, T., Zein, I., Ng, K.W., Teoh, S.H., Tan, K.C., *et al.* Mechanical properties and cell cultural response of polycaprolactone scaffolds designed and fabricated via fused deposition modeling. J Biomed Mater Res **55,** 203, 2001.
28. Iroh, J., and Mark, J. Poly(epsilon-caprolactone). In: Mark, J.E., ed. Polymer Data Handbook. New York, NY: Oxford University Press Inc., 1999, pp. 361–362.
29. Hutmacher, D.W. Scaffolds in tissue engineering bone and cartilage. Biomaterials **21,** 2529, 2000.
30. Rai, B., Teoh, S.H., Hutmacher, D.W., Cao, T., and Ho, K.H. Novel PCL-based honeycomb scaffolds as drug delivery systems for rhBMP-2. Biomaterials **26,** 3739, 2005.
31. Wozney, J.M., and Li, R.H. Engineering what comes naturally. Nat Biotechnol **21,** 506, 2003.
32. Ai-Aql, Z.S., Alagl, A.S., Graves, D.T., Gerstenfeld, L.C., and Einhorn, T.A. Molecular mechanisms controlling bone formation during fracture healing and distraction osteogenesis. J Dent Res **87,** 107, 2008.
33. Kempen, D.H.R., Lu, L., Heijink, A., Hefferan, T.E., Creemers, L.B., Maran, A., *et al.* Effect of local sequential VEGF and BMP-2 delivery on ectopic and orthotopic bone regeneration. Biomaterials **30,** 2816, 2009.
34. Yamamoto, M., Takahashi, Y., and Tabata, Y. Controlled release by biodegradable hydrogels enhances the ectopic bone formation of bone morphogenetic protein. Biomaterials **24,** 4375, 2003.
35. Uludag, H., D'Augusta, D., Palmer, R., Timony, G., and Wozney, J. Characterization of rhBMP-2 pharmacokinetics implanted with biomaterial carriers in the rat ectopic model. J Biomed Mater Res **46,** 193, 1999.
36. Uludag, H., Friess, W., Williams, D., Porter, T., Timony, G., D'Augusta, D., *et al.* rhBMP-collagen sponges as osteoinductive devices: effects of *in vitro* sponge characteristics and protein pI on *in vivo* rhBMP pharmacokinetics. Ann N Y Acad Sci **875,** 369, 1999.
37. Lee, J., Son, M.J., Woolard, K., Donin, N.M., Li, A., Cheng, C.H., *et al.* Epigenetic-mediated dysfunction of the bone morphogenetic protein pathway inhibits differentiation of glioblastoma-initiating cells. Cancer Cell **13,** 69, 2008.
38. Rai, B., Oest, M.E., Dupont, K.M., Ho, K.H., Teoh, S.H., Guldberg, R.E., *et al.* Combination of platelet-rich plasma with polycaprolactone-tricalcium phosphate scaffolds for segmental bone defect repair. J Biomed Mater Res A **81,** 888, 2007.
39. Narayan, R., ed. Biomedical Materials. Dusseldorf, Germany: Springer Verlag, 2009, 566p.
40. Wise, D.L., ed. Biomaterials Engineering and Devices: Orthopedic, Dental, and Bone Graft Applications. Totowa, NJ: Humana Pr. Inc., 2000.
41. Chen, D., Zhao, M., and Mundy, G.R. Bone morphogenetic proteins. Growth Factors **22,** 233, 2004.
42. Onishi, T., Ishidou, Y., Nagamine, T., Yone, K., Imamura, T., Kato, M., *et al.* Distinct and overlapping patterns of localization of bone morphogenetic protein (BMP) family members and a BMP type II receptor during fracture healing in rats. Bone **22,** 605, 1998.
43. Ishidou, Y., Kitajima, I., Obama, H., Maruyama, I., Murata, F., Imamura, T., *et al.* Enhanced expression of type I receptors for bone morphogenetic proteins during bone formation. J Bone Miner Res **10,** 1651, 1995.
44. Mehlhorn, A.T., Niemeyer, P., Kaschte, K., Muller, L., Finkenzeller, G., Hartl, D., *et al.* Differential effects of BMP-2

and TGF-beta1 on chondrogenic differentiation of adipose derived stem cells. Cell Prolif **40,** 809, 2007.
45. Cook, S.D., Wolfe, M.W., Salkeld, S.L., and Rueger, D.C. Effect of recombinant human osteogenic protein-1 on healing of segmental defects in non-human primates. J Bone Joint Surg Am **77,** 734, 1995.
46. Chu, T.W., Wang, Z.G., Zhu, P.F., Jiao, W.C., Wen, J.L., Gong, S.G., *et al.* [Effect of vascular endothelial growth factor in fracture healing]. Zhongguo Xiu Fu Chong Jian Wai Ke Za Zhi **16,** 75, 2002.
47. Street, J., Bao, M., deGuzman, L., Bunting, S., Peale, F.V., Ferrara, N., *et al.* Vascular endothelial growth factor stimulates bone repair by promoting angiogenesis and bone turnover. Proc Natl Acad Sci U S A **99,** 9656, 2002.
48. Kanczler, J.M., and Oreffo, R.O.C. Osteogenesis and angiogenesis: the potential for engineering bone. Eur Cell Mater **15,** 100, 2008.
49. Rai, B., Ho, K.H., Lei, Y., Si-Hoe, K.M., Jeremy Teo, C.M., Yacob, K.B., *et al.* Polycaprolactone-20% tricalcium phosphate scaffolds in combination with platelet-rich plasma for the treatment of critical-sized defects of the mandible: a pilot study. J Oral Maxillofac Surg **65,** 2195, 2007.
50. Rai, B., Teoh, S.H., Ho, K.H., Hutmacher, D.W., Cao, T., Chen, F., *et al.* The effect of rhBMP-2 on canine osteoblasts seeded onto 3D bioactive polycaprolactone scaffolds. Biomaterials **25,** 5499, 2004.

Address correspondence to:
*Hae-Ryong Song, M.D., Ph.D.*
*Department of Orthopaedic Surgery*
*Korea University College of Medicine*
*Guro Hospital*
*#80 Guro-Dong*
*Guro-Gu*
*Seoul 152-703*
*Korea*

*E-mail:* songhae@korea.ac.kr

*Swee-Hin Teoh, Ph.D.*
*National University of Singapore Tissue Engineering Program (NUSTEP)*
*Center for Biomaterials Applications and Technology (BIOMAT)*
*Department of Mechanical Engineering*
*National University of Singapore*
*9 Engineering Drive 1*
*Singapore 117576*
*Singapore*

*E-mail:* mpetsh@nus.edu.sg

*Received: January 16, 2011*
*Accepted: May 9, 2011*
*Online Publication Date: June 14, 2011*